JACS
JOURNAL OF THE AMERICAN CHEMICAL SOCIETY

Communication

pubs.acs.org/JACS

Atomically Precise Alkynyl-Protected Metal Nanoclusters as a Model Catalyst: Observation of Promoting Effect of Surface Ligands on Catalysis by Metal Nanoparticles

Yu Wang,[†] Xian-Kai Wan,[†] Liting Ren,[†] Haifeng Su,[†] Gang Li,[‡] Sami Malola,[§] Shuichao Lin,[†] Zichao Tang,[†,‡] Hannu Häkkinen,[§] Boon K Teo,[†] Quan-Ming Wang,*[,†] and Nanfeng Zheng*[,†]

[†]Collaborative Innovation Center of Chemistry for Energy Materials, State Key Laboratory for Physical Chemistry of Solid Surfaces, and Department of Chemistry, College of Chemistry and Chemical Engineering, Xiamen University, Xiamen 361005, China

[‡]State Key Laboratory of Molecular Reaction Dynamics, Dalian Institute of Chemical Physics, Chinese Academy of Sciences, Dalian 116023, China

[§]Departments of Physics and Chemistry, Nanoscience Center, University of Jyväskylä, Jyväskylä FI-40014Finland

Supporting Information

ABSTRACT: Metal nanoclusters whose surface ligands are removable while keeping their metal framework structures intact are an ideal system for investigating the influence of surface ligands on catalysis of metal nanoparticles. We report in this work an intermetallic nanocluster containing 62 metal atoms, $Au_{34}Ag_{28}(PhC{\equiv}C)_{34}$, and its use as a model catalyst to explore the importance of surface ligands in promoting catalysis. As revealed by single-crystal diffraction, the 62 metal atoms in the cluster are arranged as a four-concentric-shell Ag@Au_{17}@Ag_{27}@Au_{17} structure. All phenylalkynyl (PA) ligands are linearly coordinated to the surface Au atoms with staple "PhC≡C−Au−C≡CPh" motif. Compared with reported thiolated metal nanoclusters, the surface PA ligands on $Au_{34}Ag_{28}(PhC{\equiv}C)_{34}$ are readily removed at relatively low temperatures, while the metal core remains intact. The clusters before and after removal of surface ligands are used as catalysts for the hydrolytic oxidation of organosilanes to silanols. It is, for the first time, demonstrated that the organic-capped metal nanoclusters work as active catalysts much better than those with surface ligands partially or completely removed.

Owing to their high surface areas, metal nanoparticles have been emerged as an important class of heterogeneous catalysts for a wide range of chemical transformations.[1,2] Many parameters, including composition, size, shape, and surface structure, have been well-documented as vital factors to influence the catalytic properties of metal nanoparticles. Monodisperse metal nanoparticles having well-defined size, shape, and composition are important for studying the determining factors in catalysis and have thus attracted increasing research attention during the past two decades.[3−5] To date, the monodisperse metal nanoparticles are mainly prepared by means of colloidal chemistry which typically requires the use of surface stabilizing agents. Although the presence of surface stabilizing ligands on metal nanoparticles is considered to hinder their catalysis in most cases, an increasing number of recent studies have highlighted the importance of surface modification to enhance the catalysis by metal nanoparticles.[1,6−12] The roles of surface ligands in modulating the catalysis of metal nanoparticles are awaiting fundamental understanding.

Due to their truly monodispersity having well-defined composition and structure,[13−21] atomically precise metal nanoclusters are expected to serve as an ideal system to gain insight into the influence of surface ligands on the catalysis of metal nanoparticles.[22−26] To unambiguously identify the roles surface ligands on catalysis, it is highly desirable to prepare nanoclusters whose surface ligands are removable, while keeping their all structures intact.[27−29] Very recently, several alkynyl-stabilized metal nanoclusters with well-defined compositions or structures have been prepared.[30−36] We have demonstrated that alkynyl ligands on alkynyl-stabilized metal nanoclusters are labile enough to be readily removed under mild conditions while maintaining their overall structures.[30] Such a property of alkynyl-stabilized metal nanoclusters makes them outstanding among widely reported organic-stabilized metal nanoclusters. Thiolated metal nanoclusters typically require much higher temperatures to remove their surface ligands,[37−39] which often destroys their well-defined structures and leads to heavy aggregation during the removal process of surface ligands.[40−42]

We report herein an all-phenylalkynyl-capped intermetallic 62-metal-atom $Au_{34}Ag_{28}$ cluster, wherein the ligands can readily be removed under mild conditions, while the metal framework remains intact. The cluster has an overall composition of $Au_{34}Ag_{28}(PhC{\equiv}C)_{34}$ (**1**) with the 62 metal atoms distributed in an Ag@Au_{17}@Ag_{27}@Au_{17} form having a concentric four-shell structure. Monomeric staples (PhC≡C−Au−C≡CPh) are self-assembled into staggered pentagonal stripes on the surface of a Ag@Au_{17}@Ag_{27} kernel. The well-defined structure and lability of its surface phenylalkynyl ($PhC{\equiv}C^-$, abbreviated as PA) allow the title cluster to serve as a model system to evaluate the importance of surface ligands in catalysis of metal nanoparticles. Surprisingly, the nanocluster fully capped by PAs is demonstrated as a much active catalyst than the one with surface ligands partially or completely removed.

Received: December 6, 2015
Published: February 29, 2016

DOI: 10.1021/jacs.5b12730
J. Am. Chem. Soc. 2016, 138, 3278−3281

In a typical synthesis, $AuSMe_2Cl$ was first dissolved in the mixture solution of chloroform and methanol, after which deprotonated phenylacetylene was added (See Supporting Information (SI) for more details and also an alternative synthetic method). The suspension was stirred for 10 min, and $AgCH_3COO$ was added. After further stirring for 5 min, the reducing agent, *tert*-butylamine borane complex, was added to the mixture under vigorous stirring. The reaction was aged for 12 h at room temperature. The solvents were then removed by rotary evaporation, and the obtained products were redissolved in chloroform for crystallization. Black block crystals of **1** were obtained by solvent evaporation (yield ~28% based on Au).

The structure of **1** was determined by single-crystal X-ray diffraction and portrayed in Figure 1a and S1. The metal

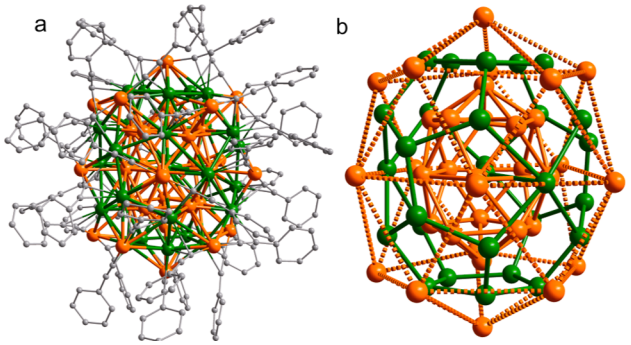

Figure 1. Crystal structure of the $Au_{34}Ag_{28}(PA)_{34}$. (a) Overall structure of the cluster. (b) Concentric four-shell $Ag@Au_{17}@Ag_{27}@Au_{17}$ framework of the 62 metal atoms in the cluster. Color codes for atoms: orange sphere, Au; green, Ag; gray, C. All hydrogen atoms are omitted for clarity.

framework can be described as an Ag centered, concentric four-shell $Ag@Au_{17}@Ag_{27}@Au_{17}$ architecture, hereafter designated as Shell-0,-1,-2, and -3, respectively (Figure 1b and S2). Shell-0 is the single core atom, Ag. Shell-1 is a hollow, distorted interpenetrating biicosahedra of Au_{17} (*vide infra*). The Au atoms in this shell have an average Au−Au bond length of 2.86 Å, comparable to the Au−Au distance (2.884 Å) in bulk face-centered cubic (fcc) gold. Shell-2 is the peculiar shell of Ag_{27} formed by capping the faces of Shell-1 (*vide infra*). It has an average Ag−Ag distance of 3.20 Å. The Au−Ag distances between Shell-1 (Au_{17}) and Shell-2 (Au_{27}) average around 2.91 Å, indicating strong metal−metal bonding between two metal shells. Shell-3 is the outermost metal shell of Au_{17}, which has an average nonbonding Au···Au distance of 5.60 Å. The disposition of atoms in Shell-3 "mirrors" those of Shell-1. There are, however, no metal−metal bonds between Shells 2 and 3 (average Au−Ag distance of 3.30 Å). Therefore, the cluster may also be described as a core−shell−shell $Ag@Au_{17}@Ag_{27}$ framework protected by an outer network of $[Au(PA)_2]_{17}$.

An ideal interpenetrating biicosahedra (*ibi*) has two icosahedral centers,[43] meaning that two atoms of the same size can be accommodated in the *ibi* cage. Instead, Shell-1 in $Au_{34}Ag_{28}(PA)_{34}$ has only one central atom and is located, unexpectedly, at the center of the middle pentagon of *ibi*. Since a planar pentagon cannot accommodate a metal atom of the same size, three of the five edges of the pentagon are lengthened significantly to 3.414, 3.865, and 3.256 Å in comparison to the two normal edges of 2.917 and 2.911 Å (Figure S3). We hereafter refer to this distortion as "equatorial distortion" or ED in short. The angles subtended by these long edges are 73, 73, and 88°, in comparison with that of 62 and 63° of the short edges. Several important structural consequences of this distortion are discussed in details in SI.

The optical absorption and electrospray ionization mass spectrometry (ESI-MS) spectra of as-prepared crude products of **1** are depicted in Figure 2a,b, respectively. The UV−vis spectrum

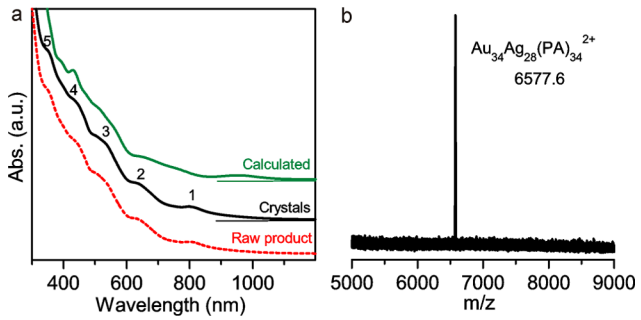

Figure 2. (a) UV−vis and (b) ESI-MS spectra of the crude product of **1**. The UV−vis spectrum of single crystals of **1** dissolved in chloroform is given in (a) for comparison.

of the crude product is identical to that of single crystals of **1**, suggesting the high-purity of **1** in the crude product. The high purity of the crude product is confirmed by a single peak of the dicationic $[Au_{34}Ag_{28}(PA)_{34}]^{2+}$ at 6577.6 m/z in Figure 2b (measured under positive-ion mode). The cluster exhibits broad and multiband features in the UV−vis region (Figure 2a). In the UV−vis absorption spectrum of **1**, five apparent peaks (at 353, 443, 528, 644, and 810 nm) are observed. Note that the absorption peaks of Au or AuAg nanoclusters of similar sizes are less pronounced (or rather featureless),[44−46] suggesting heteroatom doping and intermetallic architecture may favor discrete electronic states.

Density functional theory calculations (DFT, see details in SI) were performed to analyze the electronic structure and optical absorption of cluster **1**. The composition of **1** indicates that it has 28 "free" metallic electrons by applying the superatom counting rule (34 + 28 electrons from the metal, 34 electrons withdrawn by the ligands).[47] The frontier orbitals consist of a split 1F band and a 2S state (Figure S4). Five highest occupied states have 1F symmetry, the lowest unoccupied state has 2S symmetry, and the rest two of the 1F states follow the 2S state. The energy gap between the occupied and unoccupied states is 0.41 eV. However, due to several symmetry-forbidden transitions between the superatom states in the frontier orbital region, the true optical gap is much larger as shown below. The Ag(4d) and Au(5d) bands start to dominate the electronic structure from about 2 eV below the Fermi energy (Figure S5).

The computed optical absorption spectrum, based on the experimental crystal structure, agrees very well with the experiment (Figure 2a). All the five features seen in the experiment can also be identified in the computed spectrum (computed peaks at 392, 429, 511, 654, and 951 nm, the energy of the lowest-energy peak underestimated with respect to experiment most likely due to the choice of the DFT exchange−correlation potential). In addition, the overall shape of the computed spectrum conforms with the measured data. The analysis of transitions (explicitly shown for computed peaks 1 and 4 in Figure S6) reveals that the two lowest energy peaks 1 and 2 are superatomic transitions from 1F to 1G states. Compared to the low-energy peaks 1 and 2, the higher energy peaks 3, 4, and 5 below 600 nm start to have stronger

DOI: 10.1021/jacs.5b12730
J. Am. Chem. Soc. 2016, 138, 3278−3281

contribution from Au(5d) and Ag(4d) bands as well as from ligand state transitions. Peak 3 is the last feature that has still notable contribution also from the pure superatomic state transitions, more specifically, from 1D to 2P transitions.

Temperature-programmed decomposition/mass spectrometric was performed to investigate the thermal degradation characteristics of the alkynyl ligands on **1** (Figure 3). From

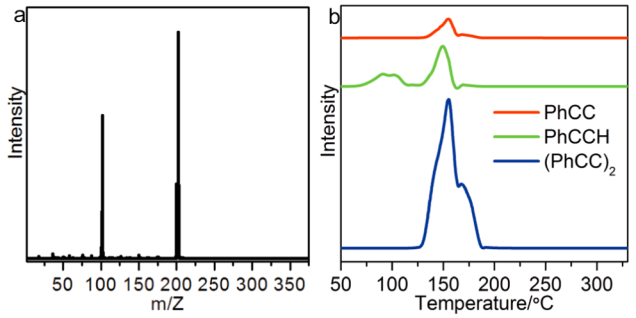

Figure 3. (a) The accumulative ionization intensity of the decomposition products of **1** from room temperature to 400 °C. (b) Relative ionization intensities of the main decomposition products of **1** upon thermal treatment under vacuum.

room temperature to 400 °C, three major decomposition products [i.e., PhC≡C (m/z = 101), PhC≡CH (m/z = 102), and $(PhC{\equiv}C)_2$ (m/z = 202)] were detected (Figure 3a). It is interesting that $(PhC{\equiv}C)_2$ dimer was not observed during the decomposition of phenylalkynyl and thiolate coprotected $Au_{24}Ag_{20}(SPy)_4(PA)_{20}Cl_2$.[30] The intensity−temperature profiles reveal that **1** underwent a rather complicated degradation process during the thermal treatment under vacuum (Figure 3b). PhC≡CH started to come out from the cluster at 60 °C, and two maximum intensities were observed at 95 and 145 °C. A small amount of PhC≡C species were also detected at 127 °C. The homocoupling product $(PhC{\equiv}C)_2$ started to release at 108 °C. Upon the thermal treatment up to 190 °C, only a trace amount of $(PhC{\equiv}C)_2$ was observed.

The cluster heated in the solid state at 100 or even 150 °C in air for 1h was still soluble in CH_2Cl_2. Almost identical absorption peak positions and intensities from its parental cluster were clearly observed in the UV−vis spectrum of the treated samples (Figure S7). And no obvious change in the particles size was observed in the TEM images of the clusters before and after the thermal treatment at 150 °C (Figure S8). These results suggested that the metal framework of the cluster remained intact after the thermal treatments. Matrix-assisted laser desorption ionization mass spectrometry analysis (Figure S9) of the thermally treated sample shows a wider signal around m/z = 11093 (assigned to fragments of **1**), indicating the loss of several alkynyl ligands on the surface of **1**. No larger nanoclusters were observed in wider range mass spectrometric analysis (e.g., from m/z 20,000 up to 80,000), although a small peak over m/z = 15,000 appeared as the laser power increased.

The above-mentioned data indicate that the metal framework remains intact, while surface ligands are partially removed upon thermal treatment at relatively low temperature. This attribute makes it possible to create reactive/active catalytic sites on the cluster surface. In this regard, we investigated the catalytic activity of **1** supported on activated carbon (XC-72) for the catalytic hydrolytic oxidation of silanes using H_2O as an oxidant. The catalytic reaction was carried out at 50 °C in acetone under air atmosphere (see SI for more details). Unexpectedly, thermally treated **1**/XC-72 had worse performances than untreated **1**/XC-72. As shown in Figure 4, **1**/XC-72 catalysts treated at 150 and

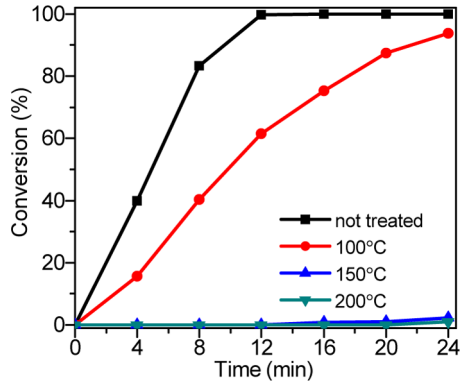

Figure 4. Catalytic performances of **1** supported on XC-72 in the hydrolytic oxidation of triethylsilane before and after thermal treatment at different temperatures.

200 °C scarcely catalyzed the reaction in the initial 12 min and gave conversions below 3% after 30 min. In contrast to the treated one, the untreated **1**/XC-72 catalyst gave 40% conversion in 4 min and 100% conversion in the following 8 min. The turnover frequency of the untreated **1**/XC-72 catalyst for hydrolytic oxidation of triethylsilane was calculated from the conversion at 4 min to be as high as 116,000 h^{-1} for each surface Au atom, which is over 3 times higher than the highest number reported in the lietrature.[48] **1**/XC-72 catalyst treated at 100 °C gave moderate performance with a 93.8% conversion in 24 min. When treated at 150 or 200 °C, **1**/XC-72 displayed negligible catalysis. But no detectable size change caused by clusters' sintering was observed on **1**/XC-72 before and after the thermal treatment at 150 °C (Figure S10). The huge difference in catalytic performances between treated and untreated **1**/XC-72 catalysts clearly suggests that, instead of being active site-blocking agents and thus catalytic poisons, surface ligands would significantly promote the catalytic activities of metal nanoparticles when designed appropriately. Again, no change was observed in the particle size of the supported nanoclusters after catalysis (Figure S11).

More importantly, the finding on the promoting effect of acetylides on catalysis was readily applied to enhance the catalysis of metal nanocatalysts. For example, **1**/XC-72 after thermal treatment at 150 °C showed negligible catalysis. Retreating the treated **1**/XC-72 with deprotonated terminal alkynes (i.e., phenylacetylene, *tert*-butylacetylene) was able to recover their catalysis to some extent (Figure S12). When TiO_2-supported Au nanoparticles prepared by the conventional deposition−precipitation method were used as the catalyst,[49] treating the catalyst with deprotonated phenylacetylene also significantly enhanced its activity (Figure S13).

In summary, an all-alkynyl-protected AuAg intermetallic nanocluster, $Au_{34}Ag_{28}(PA)_{34}$, was synthesized and structurally characterized. The structure of the cluster is unique in the following two aspects: (1) The metals are arranged in a four-shell $Ag@Au_{17}@Ag_{28}@Au_{17}$ structure, giving rise to a much featured optical absorption in the UV−vis region; (2) the monomeric staples (PhC≡C−Au−C≡CPh) are self-assembled into pentagonal stripes (staggered with respect to one another) on the quasi-spherical surface of the metallic kernel. Upon thermal treatments, $PhC{\equiv}C^-$ ligands on the cluster are easily removed at

DOI: 10.1021/jacs.5b12730
J. Am. Chem. Soc. 2016, 138, 3278−3281

relatively low temperatures, while the metal core remains intact. Carbon-supported clusters before and after removal of surface ligands were used as catalysts for the hydrolytic oxidation of organosilanes to silanols. For the first time, the organic-capped metal nanoclusters were found to exhibit far better catalytic performance than those with surface ligands partially or completely removed. It is expected that this finding would stimulate more research interests in fundamental understanding the promoting effect and applying it to optimize the catalysis by organic-capped metal nanoparticles.

■ ASSOCIATED CONTENT

Supporting Information

The Supporting Information is available free of charge on the ACS Publications website at DOI: 10.1021/jacs.5b12730.

Experimental details and data (PDF)

Crystallographic data (CIF)

■ AUTHOR INFORMATION

Corresponding Authors

*nfzheng@xmu.edu.cn

*qmwang@xmu.edu.cn

Notes

The authors declare no competing financial interest.

■ ACKNOWLEDGMENTS

We thank the MOST of China (2015CB932303) and the NSFC of China (21420102001, 21131005, 21390390, 21333008, 21473139) for financial support. The work at University of Jyväskylä was supported by the Academy of Finland (266492). The computations were made at the CSC computing center in Espoo, Finland.

■ REFERENCES

(1) Gross, E.; Somorjai, G. *Top. Catal.* **2014**, *57*, 812.

(2) Daniel, M.-C.; Astruc, D. *Chem. Rev.* **2004**, *104*, 293.

(3) Hong, J. W.; Kim, D.; Lee, Y. W.; Kim, M.; Kang, S. W.; Han, S. W. *Angew. Chem., Int. Ed.* **2011**, *50*, 8876.

(4) Wu, B. H.; Zheng, N. F. *Nano Today* **2013**, *8*, 168.

(5) Zhang, H.; Jin, M. S.; Xiong, Y. J.; Lim, B.; Xia, Y. N. *Acc. Chem. Res.* **2013**, *46*, 1783.

(6) Kahsar, K. R.; Schwartz, D. K.; Medlin, J. W. *J. Am. Chem. Soc.* **2014**, *136*, 520.

(7) Marshall, S. T.; O'Brien, M.; Oetter, B.; Corpuz, A.; Richards, R. M.; Schwartz, D. K.; Medlin, J. W. *Nat. Mater.* **2010**, *9*, 853.

(8) Wu, B. H.; Huang, H. Q.; Yang, J.; Zheng, N. F.; Fu, G. *Angew. Chem., Int. Ed.* **2012**, *51*, 3440.

(9) Dai, Y.; Liu, S. J.; Zheng, N. F. *J. Am. Chem. Soc.* **2014**, *136*, 5583.

(10) Chen, G. X.; Xu, C. F.; Huang, X. Q.; Ye, J. Y.; Gu, L.; Li, G.; Tang, Z. C.; Wu, B. H.; Yang, H. Y.; Zhao, Z. P.; Zhou, Z. Y.; Fu, G.; Zheng, N. F. *Nat. Mater.* **2016**, *16*, DOI: 10.1038/nmat4555.

(11) Taguchi, T.; Isozaki, K.; Miki, K. *Adv. Mater.* **2012**, *24*, 6462.

(12) Schrader, I.; Warneke, J.; Backenköhler, J.; Kunz, S. *J. Am. Chem. Soc.* **2015**, *137*, 905.

(13) Negishi, Y.; Nobusada, K.; Tsukuda, T. *J. Am. Chem. Soc.* **2005**, *127*, 5261.

(14) Jadzinsky, P. D.; Calero, G.; Ackerson, C. J.; Bushnell, D. A.; Kornberg, R. D. *Science* **2007**, *318*, 430.

(15) Heaven, M. W.; Dass, A.; White, P. S.; Holt, K. M.; Murray, R. W. *J. Am. Chem. Soc.* **2008**, *130*, 3754.

(16) Zhu, M. Z.; Aikens, C. M.; Hollander, F. J.; Schatz, G. C.; Jin, R. C. *J. Am. Chem. Soc.* **2008**, *130*, 5883.

(17) Desireddy, A.; Conn, B. E.; Guo, J.; Yoon, B.; Barnett, R. N.; Monahan, B. M.; Kirschbaum, K.; Griffith, W. P.; Whetten, R. L.; Landman, U.; Bigioni, T. P. *Nature* **2013**, *501*, 399.

(18) Teo, B. K. *J. Cluster Sci.* **2014**, *25*, 5.

(19) Yang, H. Y.; Wang, Y.; Huang, H. Q.; Gell, L.; Lehtovaara, L.; Malola, S.; Häkkinen, H.; Zheng, N. F. *Nat. Commun.* **2013**, *4*, 2422.

(20) Azubel, M.; Koivisto, J.; Malola, S.; Bushnell, D.; Hura, G. L.; Koh, A. L.; Tsunoyama, H.; Tsukuda, T.; Pettersson, M.; Häkkinen, H.; Kornberg, R. D. *Science* **2014**, *345*, 909.

(21) Yang, H. Y.; Wang, Y.; Yan, J. Z.; Chen, X.; Zhang, X.; Hakkinen, H.; Zheng, N. F. *J. Am. Chem. Soc.* **2014**, *136*, 7197.

(22) Chen, W.; Chen, S. W. *Angew. Chem., Int. Ed.* **2009**, *48*, 4386.

(23) Zhu, Y.; Qian, H. F.; Drake, B. A.; Jin, R. C. *Angew. Chem., Int. Ed.* **2010**, *49*, 1295.

(24) Tsukuda, T. *Bull. Chem. Soc. Jpn.* **2012**, *85*, 151.

(25) Li, G.; Jin, R. C. *Acc. Chem. Res.* **2013**, *46*, 1749.

(26) Negishi, Y. *Bull. Chem. Soc. Jpn.* **2014**, *87*, 375.

(27) Nie, X. T.; Qian, H. F.; Ge, Q. J.; Xu, H. Y.; Jin, R. C. *ACS Nano* **2012**, *6*, 6014.

(28) Xie, S.; Tsunoyama, H.; Kurashige, W.; Negishi, Y.; Tsukuda, T. *ACS Catal.* **2012**, *2*, 1519.

(29) Wu, Z. L.; Jiang, D. E.; Mann, A. K.; Mullins, D. R.; Qiao, Z. A.; Allard, L. F.; Zeng, C. J.; Jin, R. C.; Overbury, S. H. *J. Am. Chem. Soc.* **2014**, *136*, 6111.

(30) Wang, Y.; Su, H. F.; Xu, C. F.; Li, G.; Gell, L.; Lin, S. C.; Tang, Z. C.; Häkkinen, H.; Zheng, N. F. *J. Am. Chem. Soc.* **2015**, *137*, 4324.

(31) Maity, P.; Tsunoyama, H.; Yamauchi, M.; Xie, S.; Tsukuda, T. *J. Am. Chem. Soc.* **2011**, *133*, 20123.

(32) Maity, P.; Wakabayashi, T.; Ichikuni, N.; Tsunoyama, H.; Xie, S.; Yamauchi, M.; Tsukuda, T. *Chem. Commun.* **2012**, *48*, 6085.

(33) Maity, P.; Takano, S.; Yamazoe, S.; Wakabayashi, T.; Tsukuda, T. *J. Am. Chem. Soc.* **2013**, *135*, 9450.

(34) Wan, X. K.; Tang, Q.; Yuan, S. F.; Jiang, D. E.; Wang, Q. M. *J. Am. Chem. Soc.* **2015**, *137*, 652.

(35) Wan, X. K.; Xu, W. W.; Yuan, S. F.; Gao, Y.; Zeng, X. C.; Wang, Q. M. *Angew. Chem., Int. Ed.* **2015**, *54*, 9683.

(36) Wan, X. K.; Yuan, S. F.; Tang, Q.; Jiang, D. E.; Wang, Q. M. *Angew. Chem., Int. Ed.* **2015**, *54*, 5977.

(37) Zhu, Y.; Qian, H. F.; Jin, R. C. *Chem. - Eur. J.* **2010**, *16*, 11455.

(38) Zeng, C. J.; Qian, H. F.; Li, T.; Li, G.; Rosi, N. L.; Yoon, B.; Barnett, R. N.; Whetten, R. L.; Landman, U.; Jin, R. C. *Angew. Chem., Int. Ed.* **2012**, *51*, 13114.

(39) Yang, H. Y.; Wang, Y.; Lei, J.; Shi, L.; Wu, X. H.; Makinen, V.; Lin, S. C.; Tang, Z. C.; He, J.; Hakkinen, H.; Zheng, L. S.; Zheng, N. F. *J. Am. Chem. Soc.* **2013**, *135*, 9568.

(40) Gaur, S.; Miller, J. T.; Stellwagen, D.; Sanampudi, A.; Kumar, C. S. S. R.; Spivey, J. J. *Phys. Chem. Chem. Phys.* **2012**, *14*, 1627.

(41) Yoskamtorn, T.; Yamazoe, S.; Takahata, R.; Nishigaki, J.-i.; Thivasasith, A.; Limtrakul, J.; Tsukuda, T. *ACS Catal.* **2014**, *4*, 3696.

(42) Fang, J.; Li, J. G.; Zhang, B.; Yuan, X.; Asakura, H.; Tanaka, T.; Teramura, K.; Xie, J. P.; Yan, N. *Nanoscale* **2015**, *7*, 6325.

(43) Nunokawa, K.; Ito, M.; Sunahara, T.; Onaka, S.; Ozeki, T.; Chiba, H.; Funahashi, Y.; Masuda, H.; Yonezawa, T.; Nishihara, H.; Nakamoto, M.; Yamamoto, M. *Dalton Trans.* **2005**, 2726.

(44) Chaki, N. K.; Negishi, Y.; Tsunoyama, H.; Shichibu, Y.; Tsukuda, T. *J. Am. Chem. Soc.* **2008**, *130*, 8608.

(45) Chakraborty, I.; Thumu, U. B. R.; Pradeep, T. *Chem. Commun.* **2012**, *48*, 6788.

(46) Zeng, C. J.; Chen, Y. X.; Li, G.; Jin, R. C. *Chem. Mater.* **2014**, *26*, 2635.

(47) Walter, M.; Akola, J.; Lopez-Acevedo, O.; Jadzinsky, P. D.; Calero, G.; Ackerson, C. J.; Whetten, R. L.; Grönbeck, H.; Häkkinen, H. *Proc. Natl. Acad. Sci. U. S. A.* **2008**, *105*, 9157.

(48) Li, W.; Wang, A.; Yang, X.; Huang, Y.; Zhang, T. *Chem. Commun.* **2012**, *48*, 9183.

(49) Haruta, M. *Gold Bulletin* **2004**, *37*, 27.

DOI: 10.1021/jacs.5b12730
J. Am. Chem. Soc. 2016, 138, 3278−3281